

Supporting Information

Mechanism and Effects of Coverage and Particle Morphology on Rh Catalyzed NO-H₂ Reactions

Pavlo Kravchenko, Varun Krishnan, David Hibbitts*

Department of Chemical Engineering, University of Florida, Gainesville, 32611

*Corresponding author: hibbitts@che.ufl.edu

Table of Contents

S1. Abridged and Full Frequency Calculation Schemes.....	S3
Figure S1.....	S3
S2. Determination of Rotational, Translational, and Vibrational Contributions	S4
S3. NO* Filling Minimum Energy Configurations.....	S5
Figure S2.....	S5
Figure S3.....	S5
S4. N–O Scission Pathways.....	S6
Figure S4.....	S6
Figure S5.....	S7
Figure S6.....	S8
Figure S7.....	S9
Figure S8.....	S10
S4. Maximum Rate Analyses.....	S10
Figure S9.....	S11
Figure S10.....	S11
Figure S11.....	S12
Figure S12.....	S13
Figure S13.....	S13
Figure S14.....	S14
Figure S15.....	S14
Figure S16.....	S15
Figure S17.....	S16
Figure S18.....	S16
Figure S19.....	S17
Figure S20.....	S17
Figure S21.....	S18

S1. Abridged and Full Frequency Calculation Schemes

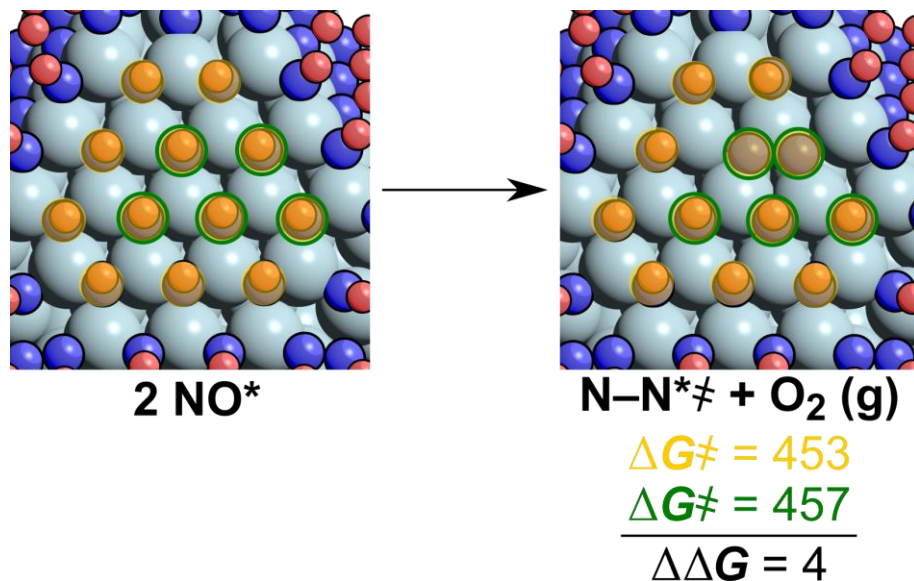


Figure S1. Calculated activation barriers (in kJ mol^{-1}) for NO^* conversion to N_2 and O_2 use two different schemes for frequency calculations. In one scheme, all adsorbates on the terrace were vibrated (in yellow), and in the other all atoms on the 3 central sites and 2 edge sites are vibrated (in green). The difference in calculated energy barriers between these models is 4 kJ mol^{-1} while the abridged scheme (in green) requires $\frac{1}{4}$ the computational resources.

S2. Determination of Rotational, Translational, and Vibrational Contributions

Enthalpies and free energies of a given state were calculated from DFT-derived potential energy (E_0), zero-point vibrational energy (ZPVE) and vibrational, translational, and rotational terms. Vibrational terms were determined using a harmonic approximation for each vibrational mode. The frequency of each mode (ν_i) was calculated using DFT. From these frequencies the zero-point free energy was calculated as:

$$ZPVE = \sum_i (\frac{1}{2} \nu_i h) \quad (S1)$$

where h is Planck's constant. Vibrational enthalpy (H_{vib}) was calculated as:

$$H_{vib} = \sum_i \left(\frac{\nu_i h e^{-\frac{\nu_i h}{kT}}}{1 - e^{-\frac{\nu_i h}{kT}}} \right) \quad (S2)$$

and free energy (G_{vib}) was calculated as:

$$G_{vib} = \sum_i \left(-kT \ln \frac{1}{1 - e^{-\frac{\nu_i h}{kT}}} \right) \quad (S3)$$

where k is Boltzmann's constant.

For surface and particle calculations rotational and translational contributions are zero, but must be taken into account for gas-phase species. The only gas molecules considered in this work are H₂ and NO, which are both linear. The rotational and translational enthalpies and free energies are calculated as:

$$H_{trans} = \frac{5}{2} kT \quad (S4)$$

$$H_{rot,linear} = kT \quad (S5)$$

$$G_{trans} = -kT \ln \left[\left(\frac{2\pi M kT}{h^2} \right)^{3/2} V \right] \quad (S6)$$

$$G_{rot} = -kT \ln \left[\frac{\pi^{1/2}}{\sigma} \left(\frac{T^3}{\theta_x \theta_y \theta_z} \right)^{1/2} \right] \quad (S7)$$

$$\theta_i = \frac{h^2}{8\pi^2 I_i k} \quad (S8)$$

where I_i is the moment of inertia about each axis (x, y, z) and σ is the symmetry factor of the molecule (2 for H₂ and 1 for NO). From these terms state enthalpy (H):

$$H = E_0 + ZPVE + H_{vib} + H_{trans} + H_{rot} \quad (S9)$$

and free energy (G):

$$G = E_0 + ZPVE + G_{vib} + G_{trans} + G_{rot} \quad (S10)$$

can be determined.

S3. NO* Filling Minimum Energy Configurations

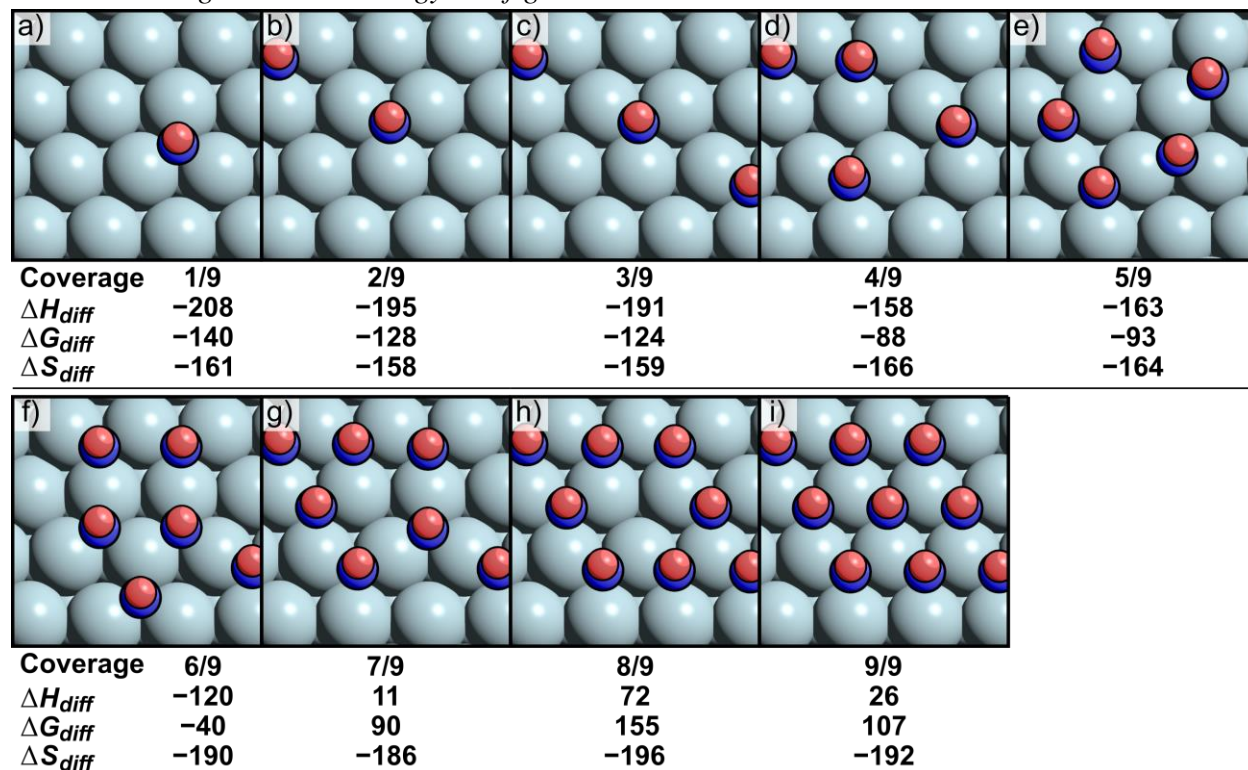


Figure S2. Minimum energy configurations of NO* covered Rh surfaces at coverages (in ML) from 1–9/9 ML. Differential adsorption enthalpies (ΔH_{diff}) and free energies (ΔG_{diff}) in kJ mol^{-1} and entropies (ΔS_{diff}) in $\text{J mol}^{-1} \text{K}^{-1}$, calculated at 423 K 1 bar.

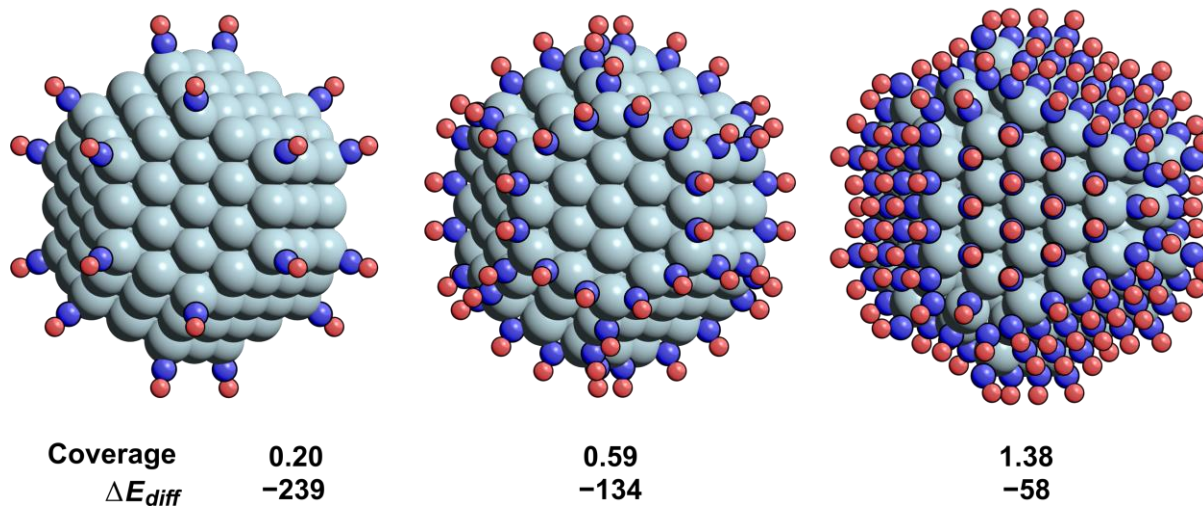


Figure S3. Minimum energy configurations for NO* covered Rh_{201} particles at intermediate coverages (in ML) ranging from 0.20–1.38 ML. Differential NO* binding energy (ΔE_{diff}) in kJ mol^{-1} .

S4. N–O Scission Pathways

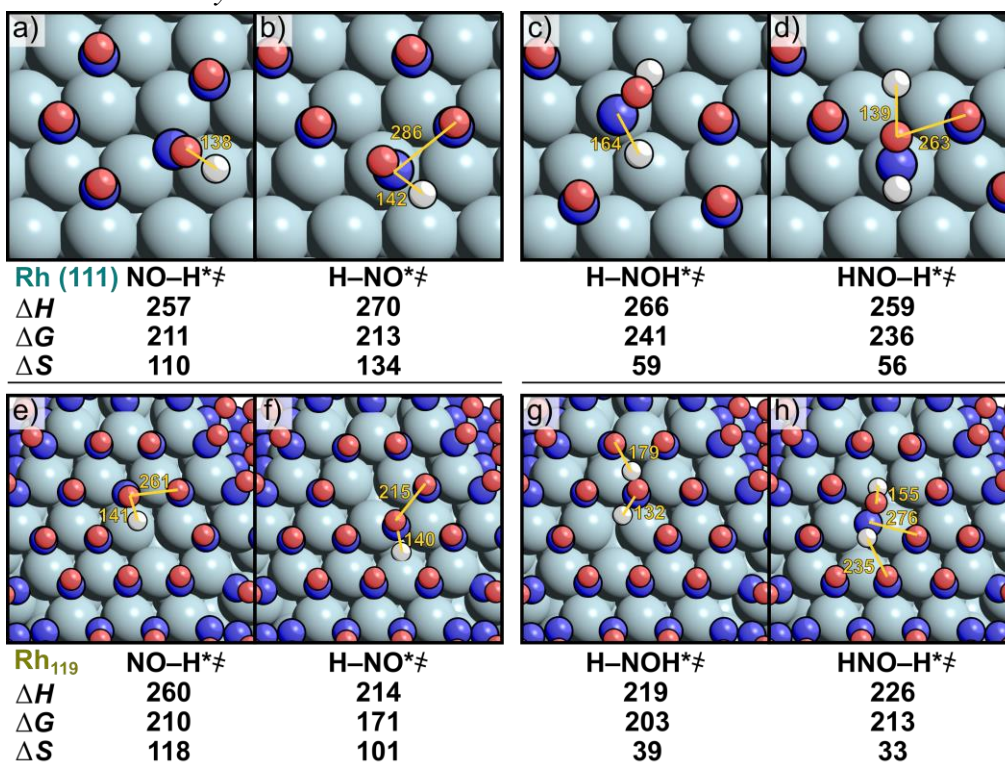


Figure S4. Structural images and enthalpies, free energies (both kJ mol^{-1}), and entropies ($\text{J mol}^{-1} \text{K}^{-1}$) to hydrogenate NO^* to NOH^* (parts **a,e**) and HNO^* (parts **b,d**) and to form HNOH^* from NOH^* (parts **c,g**) and HNO^* (parts **d,h**) at 423 K and 1 bar and 4/9 and 1.35 ML of spectating NO^* on $\text{Rh}(111)$ and Rh_{119} , respectively. Relevant distances are labeled in pm. View tilted 10° off the normal vector.

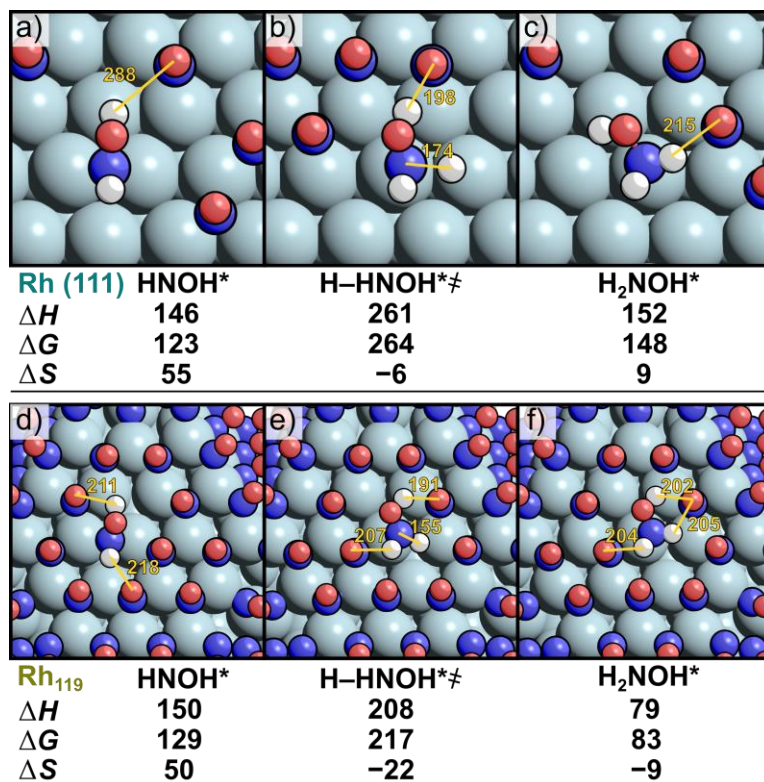


Figure S5. Structural images and enthalpies, free energies (both kJ mol^{-1}), and entropies ($\text{J mol}^{-1} \text{K}^{-1}$) of HNOH* (parts **a,d**), HNOH* hydrogenation (parts **b,e**), and H₂NOH* (parts **c,f**) at 423 K and 1 bar and 4/9 and 1.35 ML of spectating NO* on Rh(111) and Rh₁₁₉, respectively. Relevant distances are labeled in pm. View tilted 10° off the normal vector.

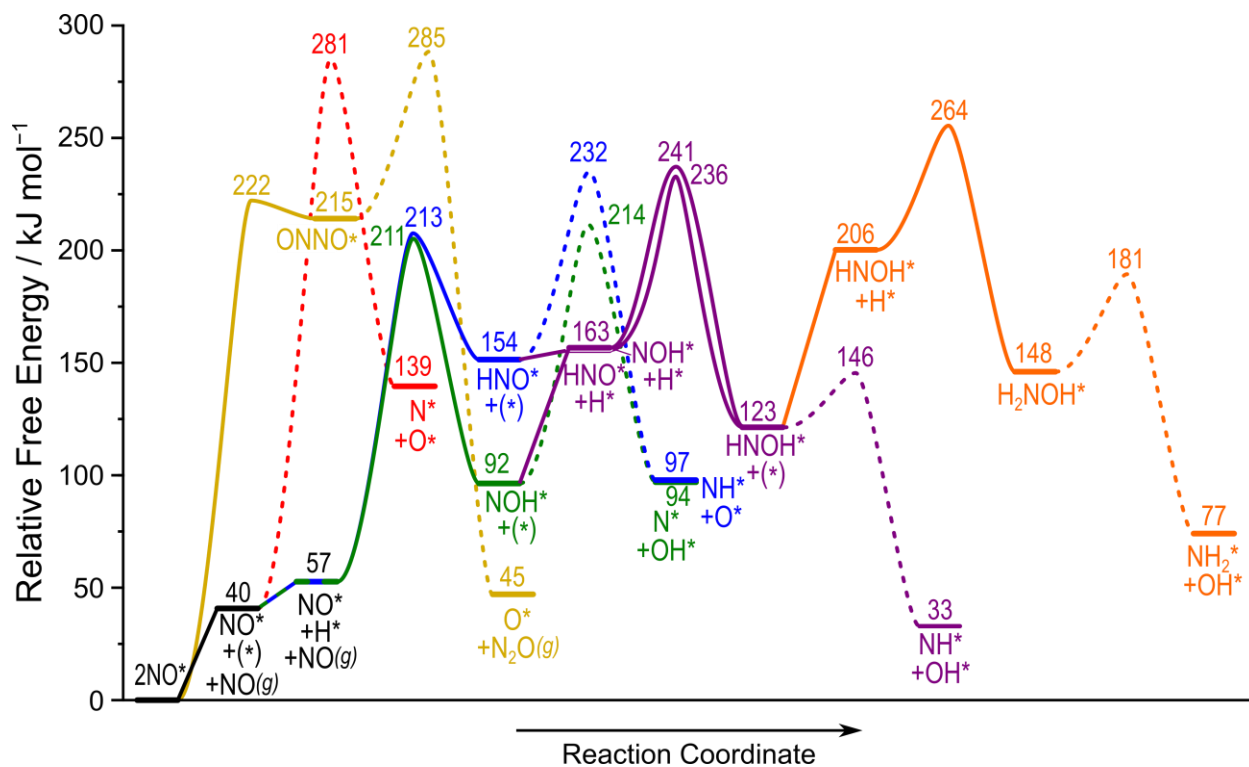


Figure S6. Comparison of NO dissociation pathways on Rh(111) (423 K 1 bar). The coverage of the initial state (denoted by 2NO^*) is 6/9 ML NO^* . Colors represent the different pathways in Scheme 1. Dashed lines indicate steps that break the N–O bond.

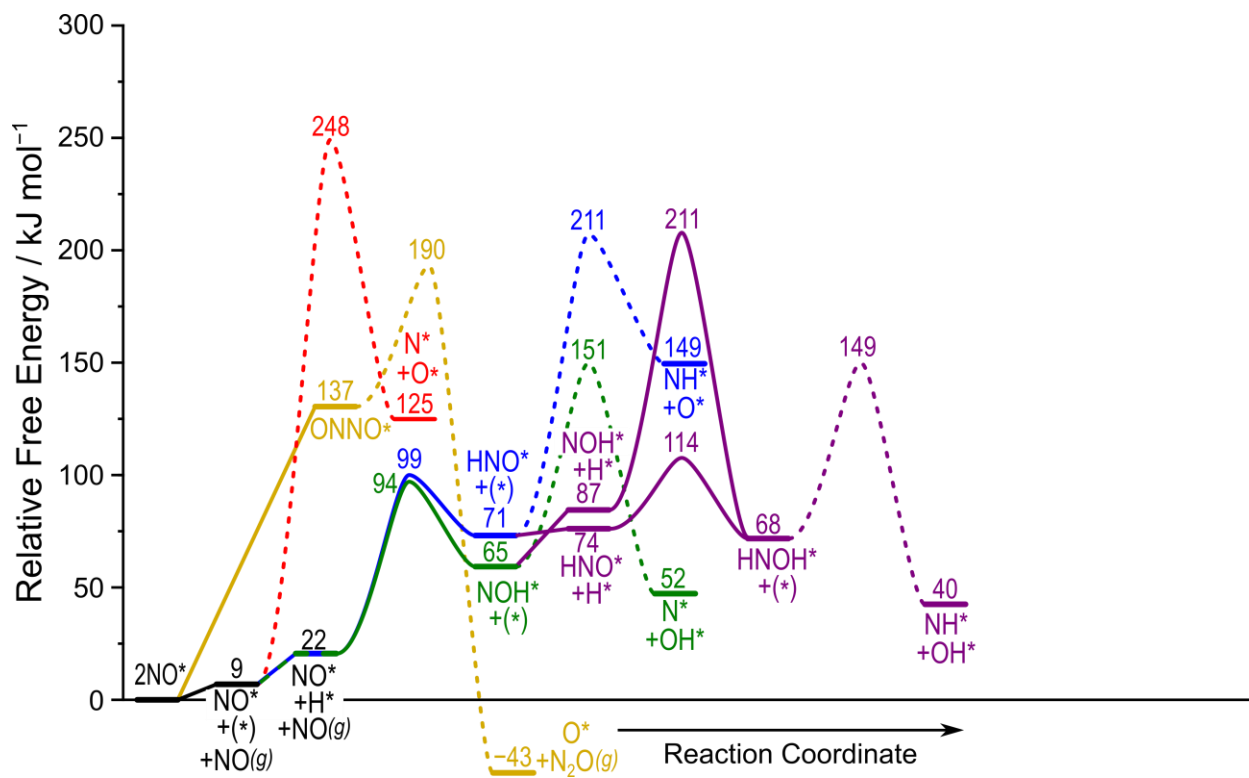


Figure S7. Comparison of NO dissociation pathways on Pt(111) (423 K 1 bar). The coverage of the initial state (denoted by 2NO^*) is 5/9 ML NO^* . Colors represent the different pathways in Scheme 1. Dashed lines indicate steps that break the N–O bond.

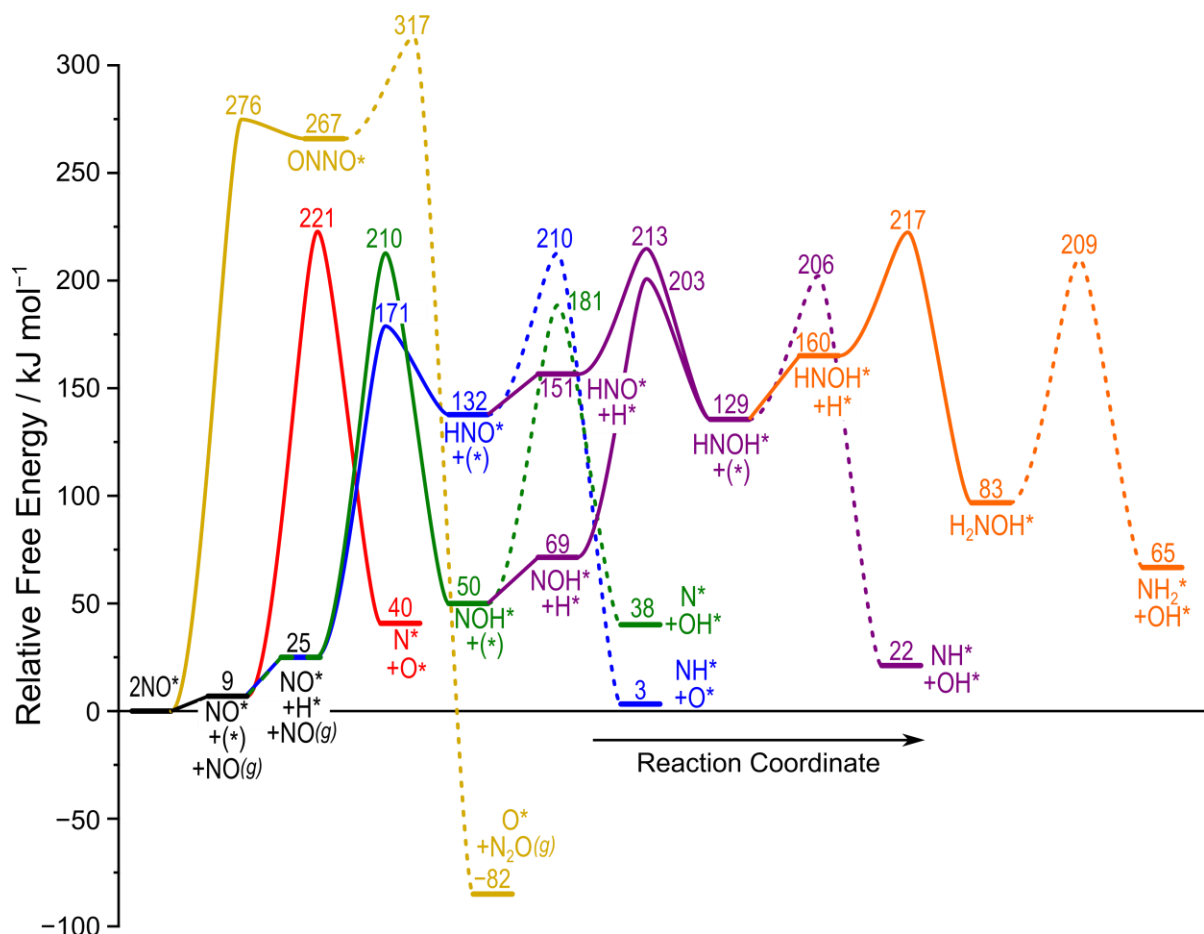


Figure S8. Comparison of NO dissociation pathways on Rh₁₁₉ (423 K 1 bar). The coverage of the initial state (denoted by 2NO*) is 1.38 ML NO*. Colors represent the different pathways in Scheme 1. Dashed lines indicate steps that break the N–O bond.

S5. Maximum Rate Analyses

Maximum rate analysis on Pt were performed for pathways 3, 4, and 5, the results of which are shown in Figs. S9–S11. Prior investigations on Pt did not model the formation of ONNO*, which is assumed to be quasi-equilibrated in this analysis. Direct NO dissociation (Pathway 2) only has one step, which the kinetically relevant step. Pathway 6 was not modeled in the previous work. The rate limiting step is HNO* dissociation (Step 3b) for Pathway 3, NOH* dissociation (Step 4b) for Pathway 4, and HNOH* dissociation (Step 5b) for Pathway 5.

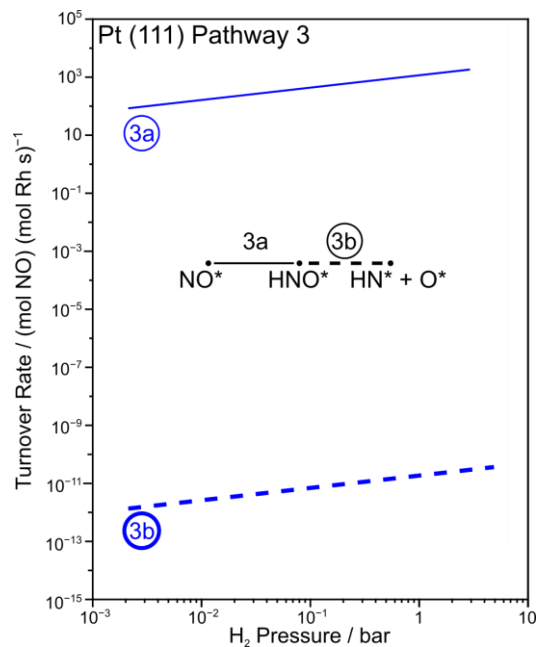


Figure S9. Maximum rate analysis and schematic representation of the formation and dissociation of HNO* on Pt(111). $P_{\text{NO}} = 0.003$ bar, $T = 423$ K. Rate determining step bolded. Colors and step numbers correspond to reaction pathways and steps in Scheme 1.

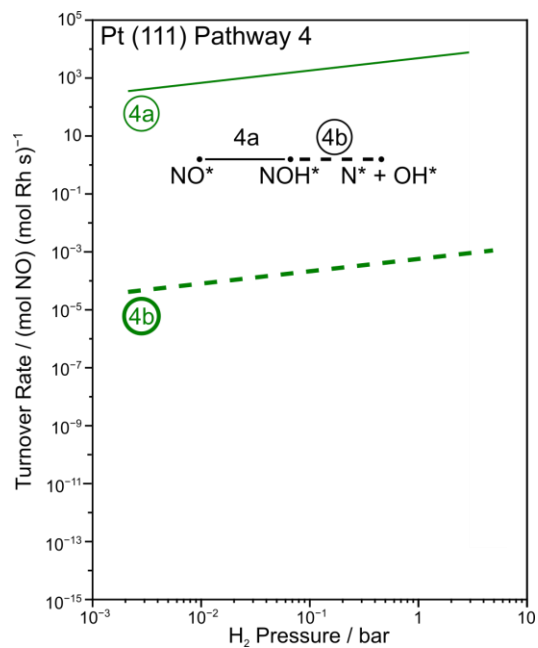


Figure S10. Maximum rate analysis and schematic representation of the formation and dissociation of NOH* on Pt(111). $P_{\text{NO}} = 0.003$ bar, $T = 423$ K. Rate determining step bolded. Colors and step numbers correspond to reaction pathways and steps in Scheme 1.

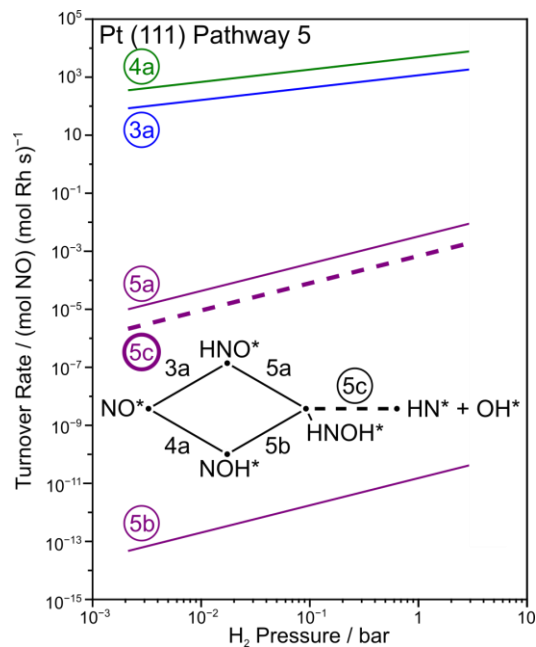


Figure S11. Maximum rate analysis and schematic representation of the formation and dissociation of HNOH* on Pt(111). $P_{\text{NO}} = 0.003$ bar, $T = 423$ K. Rate determining step bolded. Colors and step numbers correspond to reaction pathways and steps in Scheme 1.

The results of maximum rate analyses on all pathways examined on Rh(111) are shown in Figs. S12–S16. For Pathway 2 the only step (NO dissociation) is the rate limiting step. The limiting step for Pathways 1, 3, and 4 are the dissociation steps (Steps 1b, 3b, and 4b). The limiting step for Pathway 5 is the formation of HNOH* from HNO* (Step 5a), indicating this step is irreversible. Because Step 5a is irreversible, the only possible pathway for the formation and dissociation of H₂NOH (Pathway 6) is through NOH*, and the limiting step is the formation (6a).

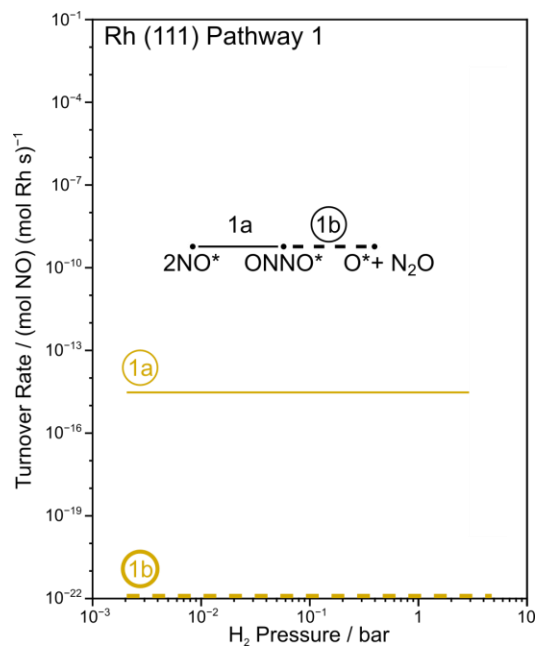


Figure S12. Maximum rate analysis and schematic representation of the formation and dissociation of ONNO* on Rh(111). $P_{\text{NO}} = 0.003$ bar, $T = 423$ K. Rate determining step bolded. Colors and step numbers correspond to reaction pathways and steps in Scheme 1.

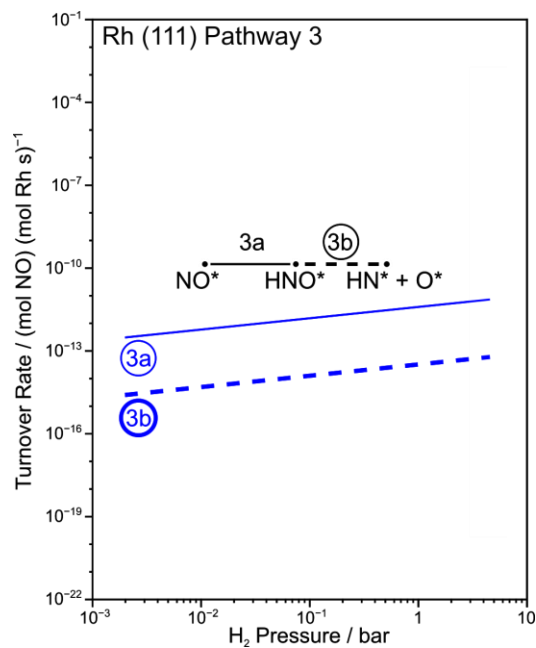


Figure S13. Maximum rate analysis and schematic representation of the formation and dissociation of HNO* on Rh(111). $P_{\text{NO}} = 0.003$ bar, $T = 423$ K. Rate determining step bolded. Colors and step numbers correspond to reaction pathways and steps in Scheme 1.

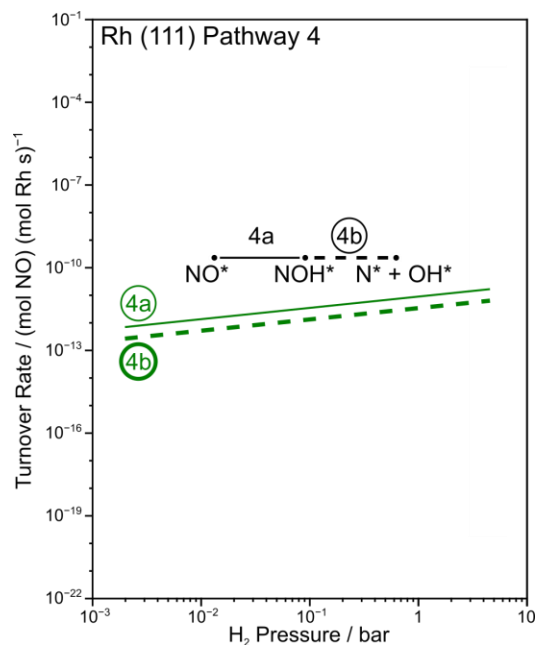


Figure S14. Maximum rate analysis and schematic representation of the formation and dissociation of NOH* on Rh(111). $P_{\text{NO}} = 0.003$ bar, $T = 423$ K. Rate determining step bolded. Colors and step numbers correspond to reaction pathways and steps in Scheme 1.

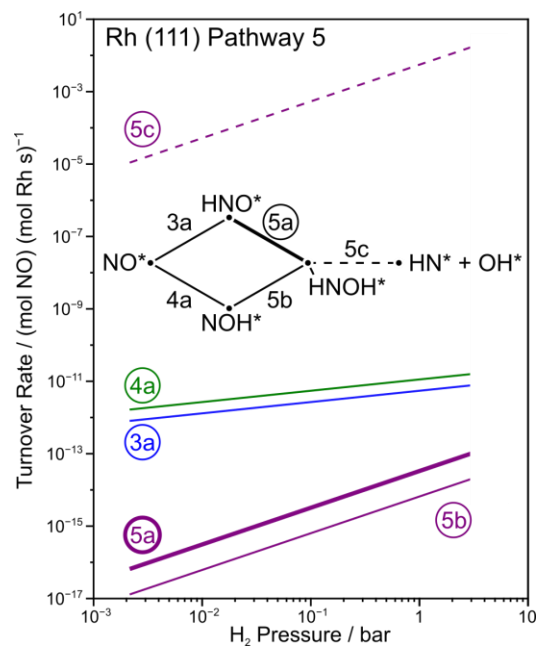


Figure S15. Maximum rate analysis and schematic representation of the formation and dissociation of HNOH* on Rh(111). $P_{\text{NO}} = 0.003$ bar, $T = 423$ K. Rate determining step bolded. Colors and step numbers correspond to reaction pathways and steps in Scheme 1.

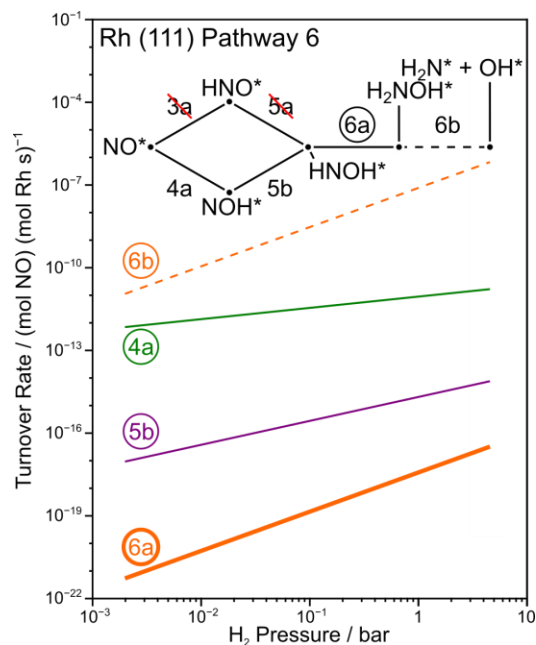


Figure S16. Maximum rate analysis and schematic representation of the formation and dissociation of H_2NOH^* on Rh(111). $P_{\text{NO}} = 0.003$ bar, $T = 423$ K. Rate determining step bolded. Colors and step numbers correspond to reaction pathways and steps in Scheme 1. Steps 3a and 5a are unavailable for the formation of H_2NOH^* as Step 5a was determined to be irreversible from the analysis done on Pathway 5.

The results of maximum rate analyses on all pathways examined on Rh_{119} are shown in Figs. S17–S21. For Pathway 2 the only step (NO dissociation) is the rate limiting step. The limiting step for Pathways 1 and 3 are the dissociation steps (Steps 1b and 3b). The limiting step for Pathway 4 is NOH^* formation (4a), indicating this step is irreversible. Because step 4a is irreversible, the rate of HNOH^* formation through NOH^* depends on the probability that NOH^* will hydrogenate and subsequently dissociation (5c) instead of dissociate (4b), which is $\sim 10^{-6}$ – 10^{-4} across the entire H_2 range. This low probability means that NOH^* will almost always dissociate and that Pathway 5 is instead limited by the formation of HNOH^* through HNO^* (Step 5a) (Figure S20). Similarly, for Pathway 6, H_2NOH^* is formed through HNO^* , and is limited by Step 6a.

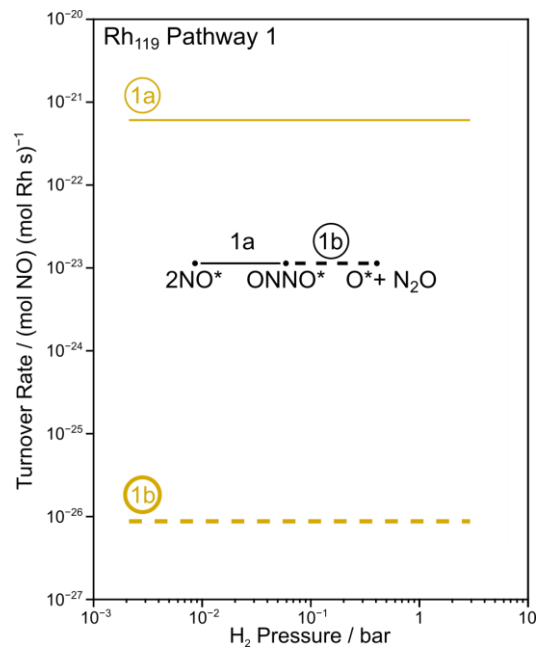


Figure S17. Maximum rate analysis and schematic representation of the formation and dissociation of ONNO* on Rh₁₁₉. P_{NO} = 0.003 bar, T = 423 K. Rate determining step bolded. Colors and step numbers correspond to reaction pathways and steps in Scheme 1.

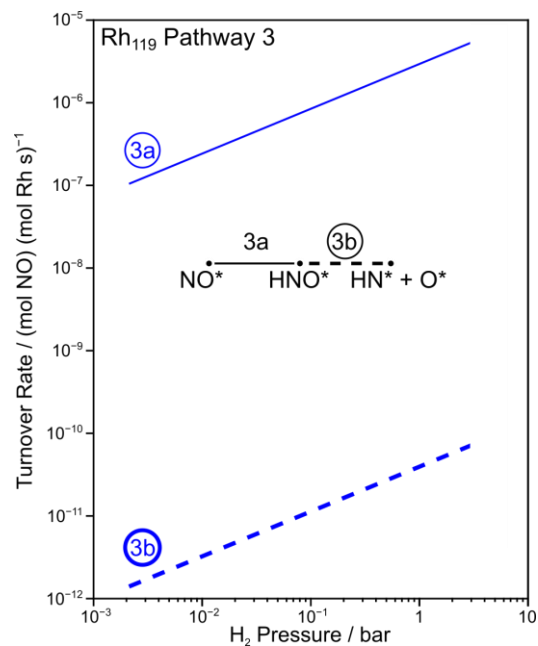


Figure S18. Maximum rate analysis and schematic representation of the formation and dissociation of HNO* on Rh₁₁₉. P_{NO} = 0.003 bar, T = 423 K. Rate determining step bolded. Colors and step numbers correspond to reaction pathways and steps in Scheme 1.

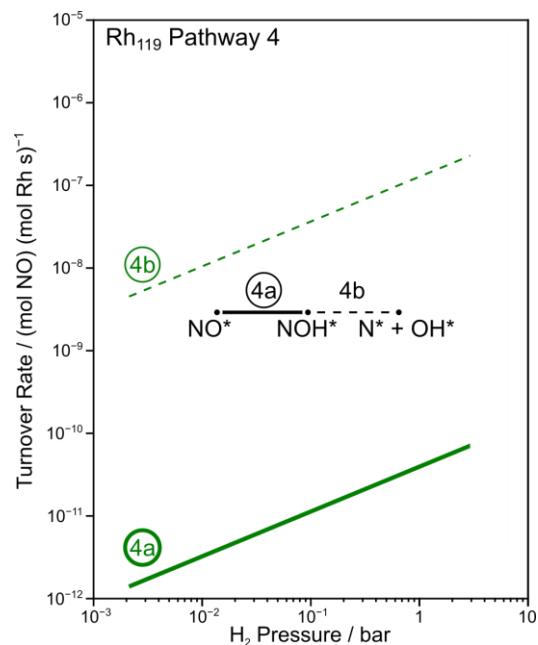


Figure S19. Maximum rate analysis and schematic representation of the formation and dissociation of NOH^* on Rh_{119} . $P_{\text{NO}} = 0.003$ bar, $T = 423$ K. Rate determining step bolded. Colors and step numbers correspond to reaction pathways and steps in Scheme 1.

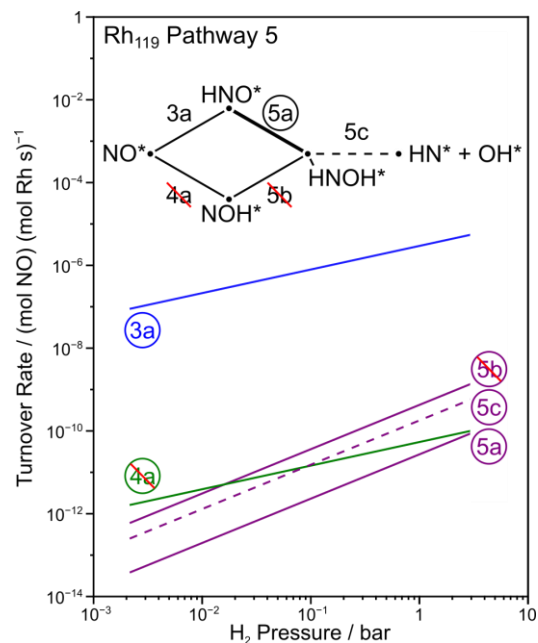


Figure S20. Maximum rate analysis and schematic representation of the formation and dissociation of HNOH^* on Rh_{119} . $P_{\text{NO}} = 0.003$ bar, $T = 423$ K. Rate determining step bolded. Colors and step numbers correspond to reaction pathways and steps in Scheme 1. Steps 4a and 5b are unavailable for the formation of HNOH^* as step 4a is irreversible and not quasi-equilibrated.

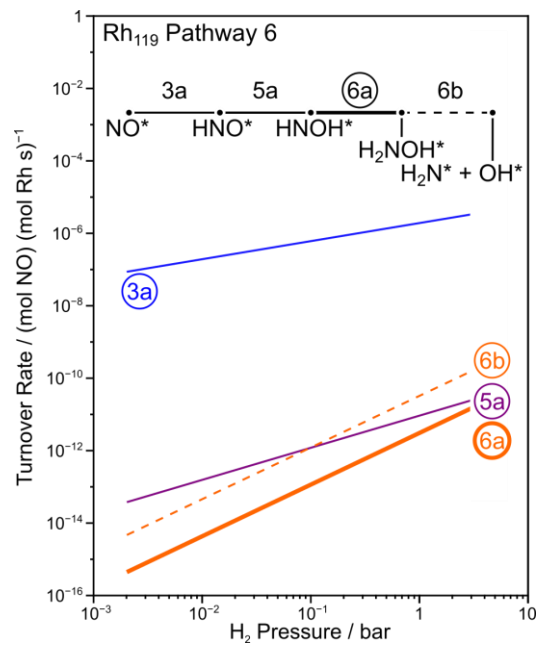


Figure S21. Maximum rate analysis and schematic representation of the formation and dissociation of H_2NOH^* on Rh_{119} . $P_{\text{NO}} = 0.003$ bar, $T = 423$ K. Rate determining step bolded. Colors and step numbers correspond to reaction pathways and steps in Scheme 1. Steps 4a and 5b are unavailable for the formation of HNOH^* as step 4a is irreversible and not quasi-equilibrated.